...rnal of Science 21A: 113-116 (2002)

...of Y_2O_3, Pd and Rh_2O_3 added in TiO_2 based sensors materials

...Malek, K.A. Ku Zarina, M. Nor Adilah and A. Isnin

...Advanced Materials Centre, SIRIM Berhad, Lot 34, Jln. Hi-Tech 2/3, Kulim Hi-Tech Park, ...Kulim, Kedah, Malaysia.

...CT X-ray diffractometry and conductivity data are used to establish the understanding of ...nsformation in titania-based sensor materials. Phase identification of titania in the anatase phase ...hase was carried out by X-ray diffractometry. The X-ray diffractometry and conductivity test of ...sed was carried-out at room temperature. The anatase structure of titania-based materials was ...dified when it was mixed with yttria, palladium and rhodium (III) oxide. It was observed that ...reased the transformation of anatase to rutile phase. However, the presence of palladium and ...(III) oxide in titania-yttria modification had slowed down the transformation of anatase to rutile. ...nce of anatase phase increased the conductivity while the rutile phase apparently inhibited the ...ity in the titania-based and titania modified based materials.

...ffractometry, Conductivity, Titania-based, Anatase phase, Rutile phase)

INTRODUCTION

...have the function of converting a ...s into a measured signal. The stimulus ...mechanical, thermal, electromagnetic, ...r, or in chemical [1]. Semiconductor gas ...is one of widely research area based on ...ity to temperature while responding to ...ations in gas composition.

...ania-based is one of the materials that had ...vestigated for gas sensor materials due to ...ility to change to different phases [2]. In ...al, the phenomenon of absorption of ...ve gases on semiconductor surface ...ficantly modifies the electrical resistance of ...aterial and this is an important property for ...detection. The anatase form of TiO_2 is used ...nse both CO and H_2 gases [3]. The first and ...most step may be assumed to be the ...ption of CO molecules on the exposed ...allite surface, express as below [4]:

$$(g) + TiO_2 \rightarrow CO_{ads}(TiO_2)$$

...is followed by the ionization of the ...orbed species on the surface, releasing a free ...ctron:

$$CO_{ads}(TiO_2) \rightarrow CO^{+}_{ads}(TiO_2) + e^{-} \quad (2)$$

Increase concentration of CO and more charge carriers (e^-) are generated. Subsequently, the resistance of the sample continues to decrease.

On the other hand,

$$CO^{+}_{ads}(TiO_2) \rightarrow CO_{ads}(TiO_2) + H^{+} \quad (3)$$

$$CO_{ads}(TiO_2) \rightarrow CO(g) \quad (4)$$

Thus, CO pressure decreases, resistance of sample increases due to desorption of CO from TiO_2 surface (see eqs. 3 and 4). The understanding of phase transformation from anatase to rutile in TiO_2 and TiO_2 modified materials for gas detection is important. This paper described the transformation of anatase to rutile for different thermal treatment of TiO_2 based materials with mixtures of yttria, palladium and rhodium (III) oxide. X-ray diffractometry (XRD) is a useful tool to characterise the phase transition of anatase to rutile due to the change of crystal structure.

EXPERIMENTAL

Commercial anatase TiO_2 (RDH, purity 99%) in the form of powder was used as starting material. The selective catalyst and dopant materials were added in weight percentage of TiO_2 and coded as in Table 1.

Table 1: Composition of titania based and titania modified based body formulations

Batch coded	Composition (wt%)			
	TiO_2	Y_2O_3	Pd	Rh_2O_3
TiO_2	100			
T-Rh_2O_3	99	-	-	1
T-Y_2O_3	90	10		
T-Y-Rh_2O_3	90	10	-	$^{+}1$
T-Y-Pd	90	10	$^{+}5$	
T-Y-P-Rh_2O_3	90	10	$^{+}5$	$^{+}1$

Note: ' $^{+}$N ' means number of percentage added into 100% of total $TiO_2 + Y_2O_3$ mixed composition.

All powder compositions in Table 1 were dried milled for 6 hours. The mixed powders were pelletised into 3mm thickness and 10mm diameter at 2 tons pressure. Pellets were dried in the oven at 100°C for 24 hours. The oven dried pellet samples were fired at temperature 800°C, 900°C, 950°C and 1000°C for 4 hours. The pellet samples are then ready for XRD analysis and conductivity test.

Conductivity Test

The conductivity of pellet samples was measured using Ultrahigh resistance meter model R8340A. 100 volt was supplied for 30s to the pellet and average value of 10 current readings were taken.

X-ray diffractometry

X-ray diffractometer system (XRD) model AXS Brunker was used for each pellet to identify the phase present. The spectra were collected at 2° per minute between 20° to 90° using CuKα radiation at 40 kV voltage and 30mA current. The JCPDS cards in database for each of the respective materials were used for comparison.

RESULTS AND DISCUSSION

The XRD analysis of the pure titania sample fired at different temperatures for 4 hours is shown in Figure 1. The samples fired at 800°C and 900°C show presence of anatase peak at 2θ=25° while the sample fired at 950°C shows mixed presence of anatase and rutile phase. Lora in her work also found that both anatase and rutile phases in titania coexisted at 950°C for 4hrs [2]. However, sample fired at 1000°C shows only presence of rutile phase at 2θ=27°. To ensure that one is working with the anatase structure, heat treatment for titania based should be below 950°C for 4hrs.

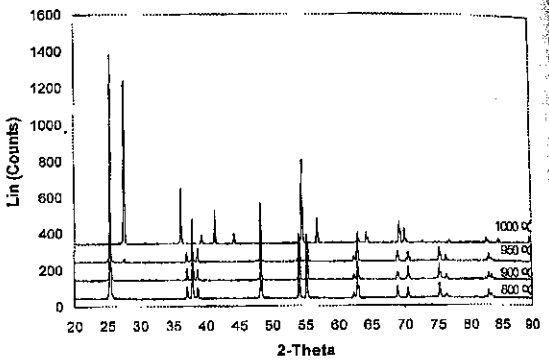

Figure 1. The XRD spectra of pure titania fired at 800°C, 900°C, 950°C and 1000°C for 4 hours.

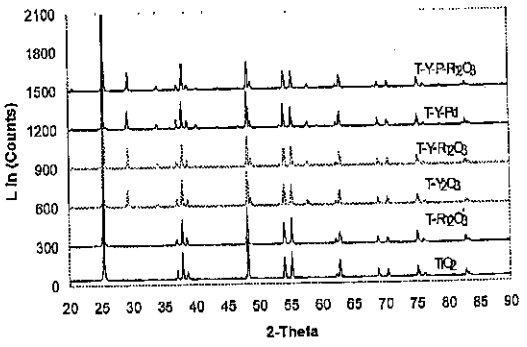

Figure 2. The X-ray powder diffraction spectra of titania based and titania modified based materials fired at 800 °C for 4 hours.

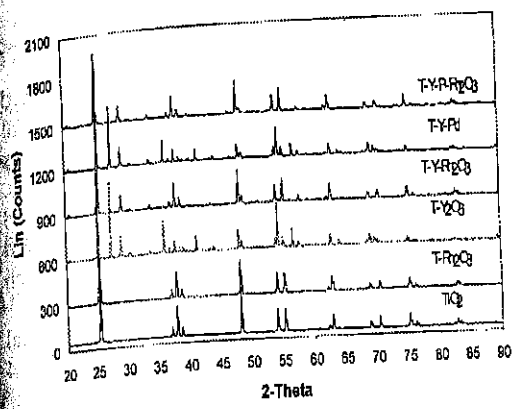

Figure 3. The X-ray powder diffraction spectra of titania based and titania modified based materials fired at 900 °C for 4 hours.

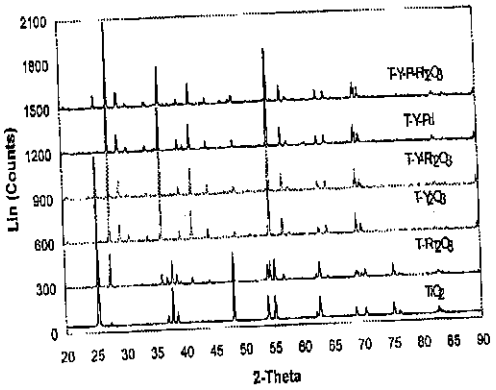

Figure 4. X-ray powder diffraction spectra of titania based and titania modified based materials fired at 950°C for 4hrs.

Figure 2 shows strong peak for anatase phase at $2\theta=25^{\circ}$ in pure titania and modified titania fired at 800 °C for 4 hours. The XRD spectrum of T-Y_2O_3 had a peak at $2\theta=29^{\circ}$ indicating presence of yttrium ion, which was incorporated in the tetragonal crystallographic system of TiO_2. At this firing temperature, no peak at $2\theta=27^{\circ}$ for rutile phase was present for all samples.

Figure 3 and Table 2 show the XRD spectra for titania and titania modified samples fired at 900 °C for 4 hours. The spectra for sample coded T-Y-Pd, T-Y-Rh_2O_3 and T-Y_2O_3 show presence of mixed anatase and rutile phase. All yttria doped titania based materials due to yttrium ion presence had influence the crystal lattice deformation and hence lower the anatase to rutile structural transformation temperature to 900 °C as indicated in Table 2.

Table 2: Phase transformation from anatase-to-rutile at different temperatures for TiO_2 and TiO_2 modified samples.

Temperature	800°C		900°C		950°C		1000°C	
Batch coded	Anatase Peak at $2\theta=$ ~25°	Rutile Peak at $2\theta=$ ~27°	Anatase Peak at $2\theta=$ ~25°	Rutile Peak at $2\theta=$ ~27°	Anatase Peak at $2\theta=$ ~25°	Rutile Peak at $2\theta=$ ~27°	Anatase Peak at $2\theta=$ ~25°	Rutile Peak at $2\theta=$ ~27°
TiO_2	Strong peak	Nil	Strong peak	Nil	Strong peak	Very small	–	Strong peak
T-Rh_2O_3	Strong peak	Nil	Strong peak	Nil	Strong peak	Medium peak	–	Strong peak
T-Y_2O_3	Strong peak	Nil	Strong peak	Strong peak	Nil	Strong peak	–	Strong peak
T-Y-Rh_2O_3	Strong peak	Nil	Strong peak	Small peak	Medium peak	Strong peak	–	Strong peak
T-Y-Pd	Strong peak	Nil	Strong peak	Medium peak	nil	Strong peak	–	Strong peak
T-Y-P-Rh_2O_3	Strong peak	Nil	Strong peak	Nil	Small peak	Strong peak	–	Strong peak

Table 3: Conductivity measured at room temperature for TiO_2 and TiO_2 modified samples fired at different temperatures.

Firing temperature	800°C	900°C	950°C	1000°C
Batch coded	Conductivity/μA	Conductivity/μA	Conductivity/μA	Conductivity/μA
TiO_2	12.91×10^3	5.40	0.80	0.54
T-Rh_2O_3	26.87	14.46	2.85	0.80
T-Y_2O_3	1.56	0.47	0.22	0.21
T-Y-Rh_2O_3	2.81	0.48	0.20	0.21
T-Y-Pd	1.89	1.01	0.25	0.25
T-Y-P-Rh_2O_3	3.23	1.20	0.72	0.39

In contrast, for TiO_2, T-Rh_2O_3 and T-Y-Pd-Rh_2O_3 samples at 900 °C for 4 hours only anatase peak at $2\theta=25°$ is present and no rutile phase peak at $2\theta=27°$. However, presence of Rh_2O_3 is seen to slow down the structural transformation to rutile even at 950 °C for 4 hours as shown in Figure 4.

Hishita et al. had reported that the anatase-to-rutile transformation is inhibited by the presence of the rare-earth oxides [5]. Figure 5 shows that at 1000°C for 4 hours all titania based and titania modified base samples are converted to rutile structure. This may be influenced by crystal growth that can be expected during thermal treatment as indicated by Emilija M. Kostic et al. [6].

Table 3 shows the conductivity value reduces as firing temperature increases from 800°C to 1000°C for pure titania and titania modified materials. Increase in deformation of anatase to rutile structure had lower down the conductivity value of all samples. For sensor material, the near insulating property of the materials cannot be used to test the sensitivity and selectivity of the targeted gas species.

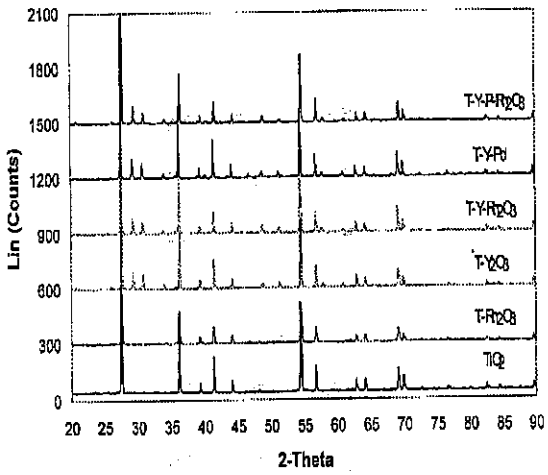

Figure 5. X-ray powder diffraction spectra of titania based and titania modified based materials fired at 1000°C for 4hrs.

CONCLUSIONS

1. The XRD spectrum for titania based materials shows that structural transformation from anatase to rutile occurs at firing temperature of 950°C for 4 hours. Based on this result, firing the titania based materials at 900°C for 4 hrs was considered to be the maximum heat treatment at which the transformation could be avoided.
2. Y^{3+} lowers down the anatase-rutile structural transformation temperature to 900°C for 4 hours in titania and titania modified samples.
3. Rh^{3+} is seen to slow down the anatase-rutile structural transformation in titania and titania modifiedsamples.
4. The conductivity values of all samples were decreased as firing temperatures increased.

Acknowledgment The authors would like to acknowledge the help of Mr. Kasfi and Mr. Abdul Rahim for the samples fabrication and conductivity measurement respectively. This work was supported by the IRPA grant: 090101-2004 (Intelligent electronic noses for in-situ monitoring of HCs, CO and NOx in automotive exhaust).

REFERENCES

1. Shieh, J., Huber, J.E., Fleck, N.A. and Ashby, M.F. (2001). *Progress in Materials Science,* **[46]** 461-504.
2. Younkman, L.B. (1995). *PhD Thesis The Ohio State University.*
3. Akbar, S., Wang, C.C. and Wang, L. (1996). *Ceramic Industry.*
4. Lora, D. B., Azad, A.M. and Akbar, S. (1992). *J. Am. Ceram. Soc.* **[75]** 2966-2968.
5. Azad, A.M. Youkman, L.B. and Akbar, S.A. (1994). *J.Am Ceram Soc.* **77**[2] 481-486.
6. Emilija, M.K., Sandor, J.K., Snezana B.B. and Slavica P.Z. (1997). *The American Ceramic Society Bulletin,* **76** [6].